JOURNAL OF THE BALKAN GEOPHYSICAL SOCIETY, Vol. 13, No. 2, December 2010, p. 21-28, 9 figs

Delineation of gypsum/anhydrite transition zone using electrical tomography. A case study in an active open pit, Altsi, Crete, Greece

Emmanouil Manoutsoglou*, George Vachlas, George Panagopoulos and Hamdan Hamdan

[1] Department of Mineral Resources Engineering, Technical University of Crete, 73100 Chania, Greece

*emanout@mred.tuc.gr

(Received 5 August 2010; accepted 20 October 2010)

Abstract: *A well known problem in the grinding procedure, in active gypsum open pits, is the difference of mechanical properties between gypsum and anhydrite. Specifically, the lower stiffness of gypsum compared to that of anhydrite, causes different energy requirements in cement production line. For these reasons it is necessary to be aware of the spatial distribution of these rocks in an active open pit. In this paper, the 2D resistivity method, in combination with detailed geological mapping, is tested as tool for the mapping of gypsum/anhydrite transition zones. A series of geophysical profiles were scanned in selected locations, following the geological mapping of the mine site, in order to locate gypsum/anhydrite transitions. In addition, the contacts of the deposit with the underlying schist formation were delineated. The results from the geophysical survey will be compared with the data from the geological mapping and the drills performed in 1982 during the exploration of the active gypsum open pit of INTERBETON S.A. in Altsi (Sitia region, Eastern Crete). This knowledge, because of its strict connection with the calculation of the reserves (geological and recoverable), contributes to the optimal production planning of the open pit.*

Key words: *Gypsum, Anhydrite, Electrical Tomography, Altsi.*

INTRODUCTION

Gypsum has extent applications in several fields, such as engineering, agriculture, cement and plaster manufacturing. In cement industry, calcium sulfate (either in the form of gypsum or anhydrite), is one of the ingredients of Portland cement which increases the time needed for the setting of cement. The difference in stiffness of anhydride and gypsum can cause problems in crushing and grinding procedure in the open pit. The stiffness of Anhydrite is 3-3.5 in Mohs scale, while for gypsum is 1.5-2. These two minerals are common in evaporitic sequences, which are deposits created by salt precipitation from aqueous solutions during solar vaporization. The precipitation begins when the aqueous solution's salt concentration exceeds 50‰ (brine). If the brine is saturated in SO_4^{-2} and Ca^{+2} gypsum or anhydrite is formed. Each of these calcium sulfate minerals usually transforms to the other one (Warren, 2006). In nature, the hydration of anhydrite to gypsum, i.e. the gypsification of anhydrite, is a frequent phenomenon (e.g. Garcia-Ruiz et al., 2007). The gypsum is dehydrated and transformed to anhydrite as a consequence of geological burial. On the contrary, anhydrite can be hydrated to gypsum when it is in contact with fluids during exhumation.

According to Holliday (1970), there are three main processes through which secondary gypsum is formed : (a) anhydrite dissolution followed by gypsum precipitation, with potential volume increase, (b) direct hydration of anhydrite, which leads to a volume increase of about 40%, and (c) stepwise hydration of bassanite ($CaSO_4½\ H_2O$). From the above, the first one is a more plausible mechanism on the Earth's surface (Pina, 2009), while the second one is mainly connected with the subsurface conditions (Warren, 2006).

Any information about the quantitative spatial distribution of these two extreme members is considered essential, both for the immediate and long term programming of an active gypsum open pit. Such information can be provided using geophysical methods, namely the 2D resistivity method, which gives the distribution of resistivity in the subsurface. These two rocks are characterized by a different range of resistivities, since gypsum lattice hosts water molecules ($CaSO_4.2H_2O$), unlike anhydrite ($CaSO_4$).

Different geophysical methods have been utilized in gypsum quarry in the past, mainly to detect main cracks or cavities (Derobert and Abraham, 2000, Ulugergerli and Akca, 2006). In this paper however, electrical tomography is used to characterize the quality of gypsum, by means of

separating gypsum from anhydrite. The differences between gypsum and anhydrite resistivities are expected to give a good picture about their spatial distribution.

GEOLOGICAL SETTING

Permian/Triassic evaporites form almost 35% of the global evaporite deposits. In that period palaeogeography and climate produced favorable circumstances for the formation of evaporites, which reached a peak during Triassic. Following the formation of Pangea and the drop of sea level, the marginal basins became shallower and a large number of endocratonic basins were created. During Permian, the climate became even more arid, contributing to the increase of evaporation's rate (Trappe, 2000). Evaporites of External Hellinides comprise a part of the Permian/Triassic evaporitic layers which were formed around Pangea. Evaporites are regarded as the first Alpine deposits of Paxos and Ionian isopic zones. This conclusion is based on field observations, compounded with existing drilling data. Their age is Permian/Triassic, but there are observations of evaporitic intercalations within limestones of lower Liasic and Cretaceous age, as well. Their thickness is more than 3000m (Rigakis and Karakitsios, 1998).

The island of Crete exhibits several sulfate outcrops. Many of them were characterized as exploitable deposits and some are still regarded as significant deposits both quantitatively and qualitatively. Those deposits are discriminated according to their time of genesis in Permian/Triassic and Neogene. The main characteristic of Neogene deposits is the exclusive existence of dihydrate form of calcium sulphate ($CaSO_4.2H_2O$) related to the "salinity crisis" or "Messinian event", which affected the whole Mediterranean area during Messinian (Kanaris, 1989). On the contrary, Permian/Triassic deposits exhibit the two main forms of calcium sulfate: gypsum ($CaSO_4.2H_2O$) and anhydrite ($CaSO_4$) (Papastamatiou, 1958, Fytrolakis, 1980, Antoniou, 1987). Deposits of Permian/Triassic age are all over the island. One of the most significant is that of Altsi in Eastern Crete. Its extent is 1.25 km^2 and is an exploitable mineral resource. It is placed above the lower layers of the metamorphic Phyllitic Nappe and it is surrounded by multi-folded schists, which belong to the same nappe, and by younger sediments as well (Kanaris, 1989).

METHODS

Geological mapping

A detailed geological mapping (scale 1:500) was conducted in the active gypsum open pit of INTERBETON S.A. in Altsi. All the geological features observed on the pit's slopes were mapped based on their macroscopic characteristics. According to this mapping, the sulfate deposit of Altsi consists of seven different lithological units, namely: (a) the schists of the bedrock, (b) the light-colored sulfates with dolomitic segments, (c) the light-colored sulfates with dark laminas, (d) the dolomites, (e) the anhydrites, (f) the soft gypsums and (h) the stiff gypsums. Representative samples were taken from each lithological unit and were analyzed geochemically. Lithological units that had similar mineralogical composition were grouped in order to simplify the geological map. This resulted in the generation of a new geological map (Fig. 1) distinguishing four lithological units. These are (1) gypsum, (2) anhydrite, (3) dolomite and (4) schist.

The geological map of Figure 1 shows the surface distribution of gypsum and anhydrite on the slopes of the open pit. Gypsum outcrops mostlycover the pit, while anhydrite outcrops in its northern and western part. The dolomitic segments are dispersed throughout the open pit, having size of centimeter to meter. The size and the frequency in appearance of dolomitic segments increase towards the upper levels of the eastern part. The bedrock is observed in the lower level of the pit.

Geophysical survey

The geophysical survey comprises of four electric tomography (ERT) lines in selected locations within the mine. Two lines (Fig. 1) were scanned using the dipole – dipole and the Wenner – Schlumberger arrays, to locate lateral gypsum – anhydrite transition, while the rest two lines were scanned only with the Wenner – Schlumberger array. The lateral resolution of the dipole – dipole array is better than the one of the Wenner – Schlumberger array, which gives better resolution in the vertical direction (Ward 1989). Electrical tomography along the third line was performed in order to locate the contact of the deposit with the underlying schist formation in the lower levels of the mine site. The fourth line is located in an active bench of the mine where one can verify the results of the geological mapping which suggest that the area consists of gypsum.

The ERT data acquisition was accomplished using the StingR1/Swift AGI system, and 27 electrodes. To ensure good contact resistances a simple drill was used to open electrode holes on the massive gypsum rock. The inversion of the apparent resistivity data was carried out using RES2DINV program. The smoothness constrained inversion (DeGroot-Hedlin and Constable, 1990) and the robust method or the L1-norm method (Claerbout and Muir, 1973) were applied. For the first two ERT lines, a mixed array inversion of the Wenner-Schlumberger and dipole-dipole arrays was employed. The result of this inversion technique usually combines Wenner-Schlumberger strong signal/noise ratio and sensitivity to vertical changes with the dipole - dipole high sensitivity to lateral changes, achieving the maximum subsurface information and the optimum arrays sensitivity (Zhou et al., 2002, Athanasiou et al., 2003, Stummer et al., 2004).

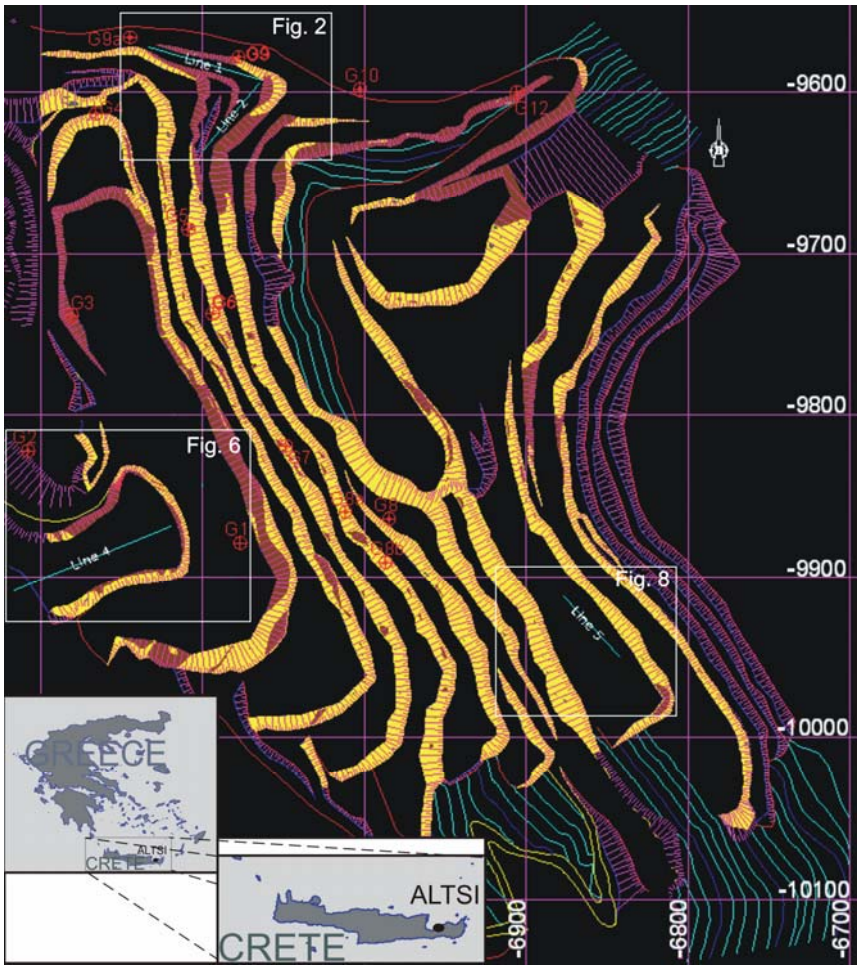

FIG. 1. Geological formations observed on the pit's slopes. Yellow: gypsum, brown: anhydrite. In addition, this map shows the position of four electric tomography lines and fourteen boreholes.

GEOPHYSICAL SURVEY RESULTS

ERT lines 1 & 2

The sections Line 1 and Line 2 are presented together because they were performed in order to map a lateral transition of gypsum to anhydrite. They scan the same bench at altitude of 242 m but in different directions. Line 1 was addressed in ESE – WNW direction (52 m long at 2 m electrode spacing), while the direction of Line 2 is NE – SW (78 m long at 3 m electrode spacing). Their target was to map a lateral anhydrite "wedge" within gypsum initially observed during the geological mapping. Figure 2 depicts the location of the anhydrite "wedge" as it was documented during the geological mapping. Gypsum is illustrated with yellow color, anhydrite with brown while dolomitic masses are gray. The ERT lines are shown in light blue. Figure 3 shows a picture of the bench where ERT lines 1 & 2 are located.

Figure 4 displays resistivity sections from the smoothness constrains inversion for the (a) Wenner-Shlumberger array, (b) the dipole-dipole array and (c) the mixed array. This type of inversion was chosen over L1-norm method, since the transition from gypsum to anhydrite is expected in a smooth manner. A shallow geoelectric layer of lower resistivity values (2 – 3 KΩm) corresponds to areas of increased ground humidity. The high values of resistivity (> 20 KΩm) are attributed to anhydrite while the intermediate values to gypsum.

In the Wenner – Schlumberger section (Fig. 4a), a geoelectric layer of high resistivity values is detected along the survey line, at depths of 2-3 m, and is contributed to anhydrite. The same high resistivity zone is observed in the dipole-dipole section (Fig. 4b), although it is not presented as a massive layer as above, but separated into four discrete zones. The boundaries of the anhydrite high resistivity zones are imaged better in the mixed array inversion results (Fig. 4c). The differences between the three sections can be attributed to the different sensitivity of each array to the lateral resistivity changes.

Borehole G9 is superimposed on the mixed array section (Fig. 4c), taking into consideration the altitude differences between the borehole bench and the tomography line bench. It is clear that the intermediate resistivity zone (5 to 7 kΩm) corresponds to the transition zone between the gypsum and the anhydrite in the borehole. The gypsum observed in the borehole underneath the transition zone, gives lower resistivity values (3 – 5 kΩm) according to the tomography section. Such resistivity values exist at the end of the line, forming a wedge which goes underneath the anhydrite mass as shown in Figure 4c (dotted black line), confirming the results of the geological mapping.

Respectively, Figure 5 displays the smoothness constrained inversion results for line 2. The shallow lower resistivity zone appears to have smaller thickness compared to line 1. Two main bodies of anhydrite are detected (black ellipse), where the first one is observed at a depth of 3-9 m (horizontal distance 20-36 m), while the second one is deeper (9-15 m). This is in agreement with the geological mapping (Figure 3), where a main mass of anhydrite is observed at horizontal distance 20-30 m. On the other hand, at the middle of the tomography line, the gypsum outcrop observed on the slope, seems to have a wider extension than concluded from the geological map.

ERT line 4

Line 4 ,located at the lowest level of the mine at an altitude of 185 m and is 130 m long (5 m electrode spacing). It was developed in a NE – SW direction. This location was selected to investigate the schist basement depth, which outcrops a few meters to the north of this line (Fig. 6). The Wenner-Shlumberger array was utilized for this purpose. Figure 7 displays the smoothness constrained (a) and the L1-norm (Robust) (b) inversion results for ERT line 4. In this case, where sharp boundaries between schist and gypsum are expected, the L1-norm inversion section is considered more reliable.

In the tomography sections of line 4 (Fig. 7), the dominant resistivity is less than 1.5 kΩm, which most likely corresponds to the schist formation. This is supported from the observations during the geological mapping of the mine, where the schist also outcrops in the upper bench. Additionally drilling data confirm the existence of the schist formation at these depths. More specifically, at borehole G2 located 150 meters NW of the survey site, the depth of the schist is 10 meters hosting gypsum in forms of small veins and thin layers. Such gypsum occurrences can be observed in the tomography section as higher resistivity zones (3 – 7 kΩm).

ERT line 5

The fourth survey line located in an active bench of the mine at an altitude of 318 m is 52 m long (2 m electrode spacing). The purpose of this survey line was to confirm the results of the geological mapping, according to which this position contains only gypsum along with small scarce dolomite fragments. Due to technical problems, only Wenner – Schlumberger array was applied in this line. The location of this line is illustrated in Figure 8. Figure 9 displays the smoothness constrained (a) and the L1-norm (Robust) (b) inversion results for ERT line 5. As expected, the resistivity values indicate that most parts of this profile consist of gypsum. However, a zone of high resistivity values is detected in the middle of the survey line, at a depth of 7 – 8 m, which indicates the presence of anhydrite mass within the main gypsum body.

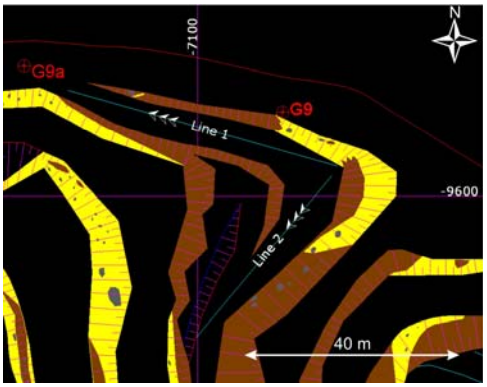

FIG. 2. A part of the geological map (Fig.1) of the quarry and the location of ERT lines 1 & 2. Grey colour indicates dolomite pieces.

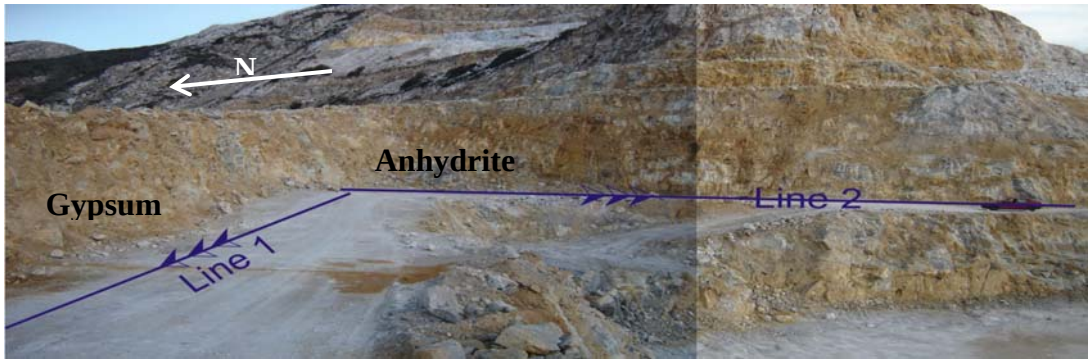

FIG. 3. A picture of the bench where ERT lines 1 & 2 took place.

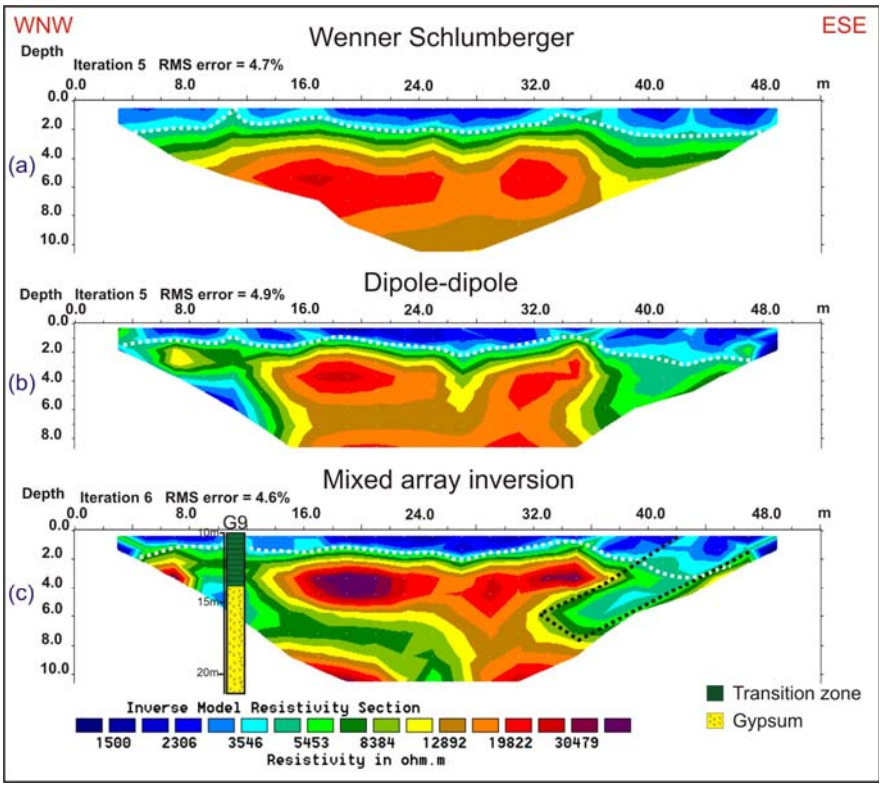

FIG. 4. Geoelectric sections for Wenner-Schlumberegr array (a), Dipole-dipole array (b) and mixed array (c) of line 1. The dotted black line depicts a gypsum wedge lying underneath the anhydrite mass.

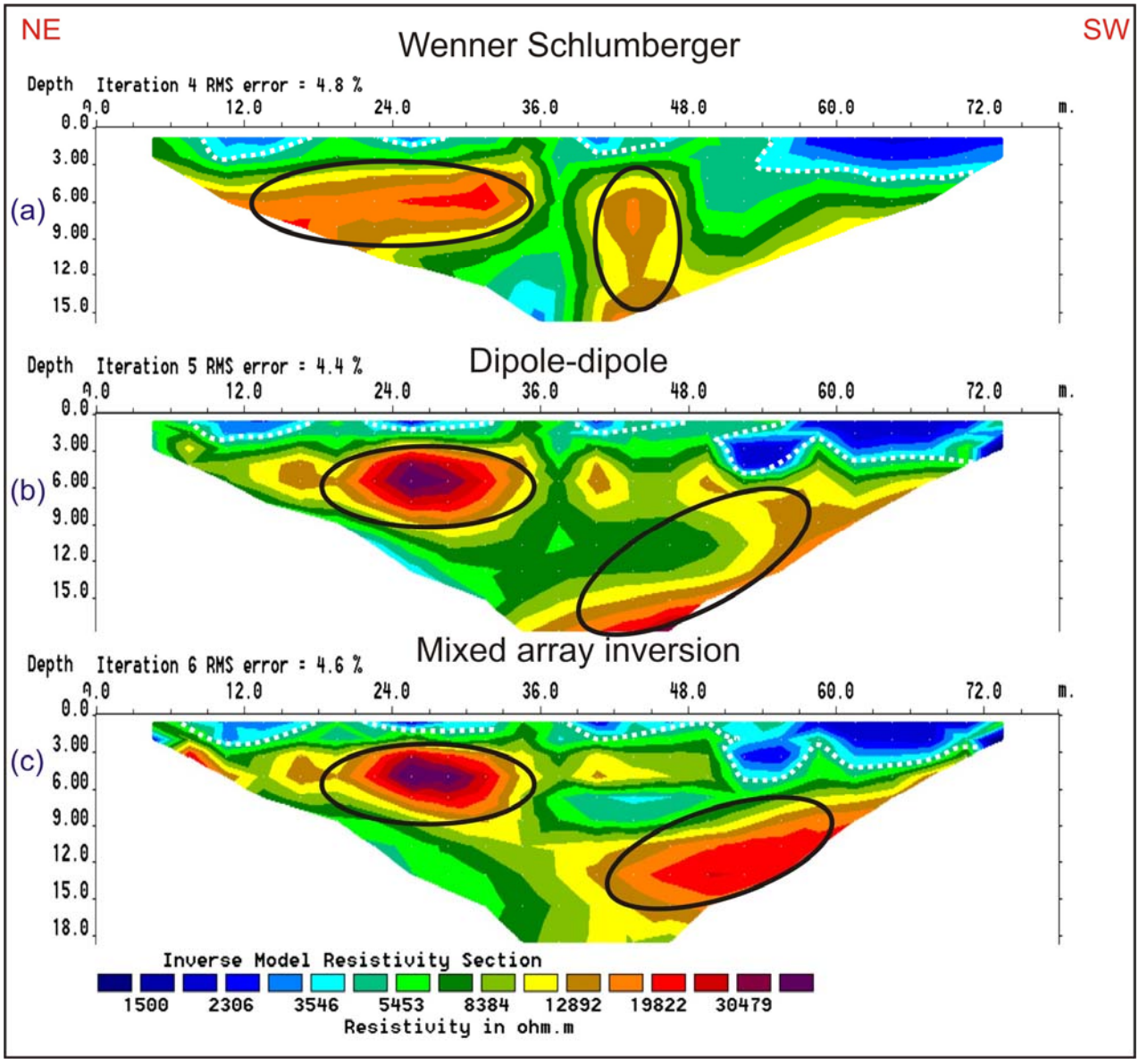

FIG. 5. Geoelectric sections for Wenner-Schlumberegr array (a), Dipole-dipole array (b) and mixed array (c) of line 2. The black ellipse depicts the anhydrite bodies.

FIG. 6. A part of the geological map (Fig.1) of the quarry and the location of ERT line 4. Red colour indicates the schists (bedrock).

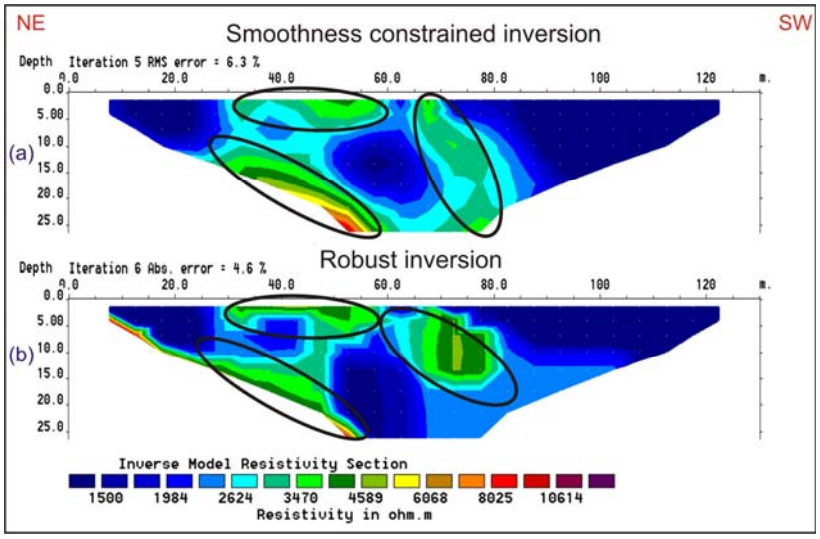

FIG. 7. Geoelectric section for line 4 using the smoothness constrained (a) and the robust (b) inversion.

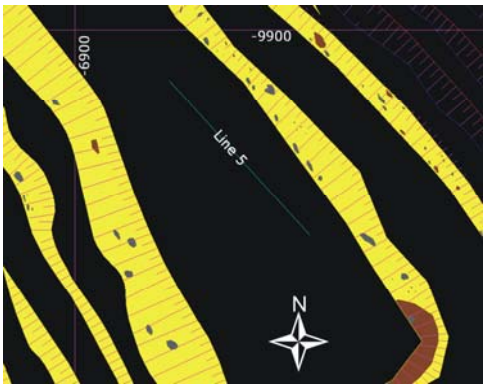

Fig. 8. A part of the geological map (Fig.1) of the quarry and the location of ERT line 5.

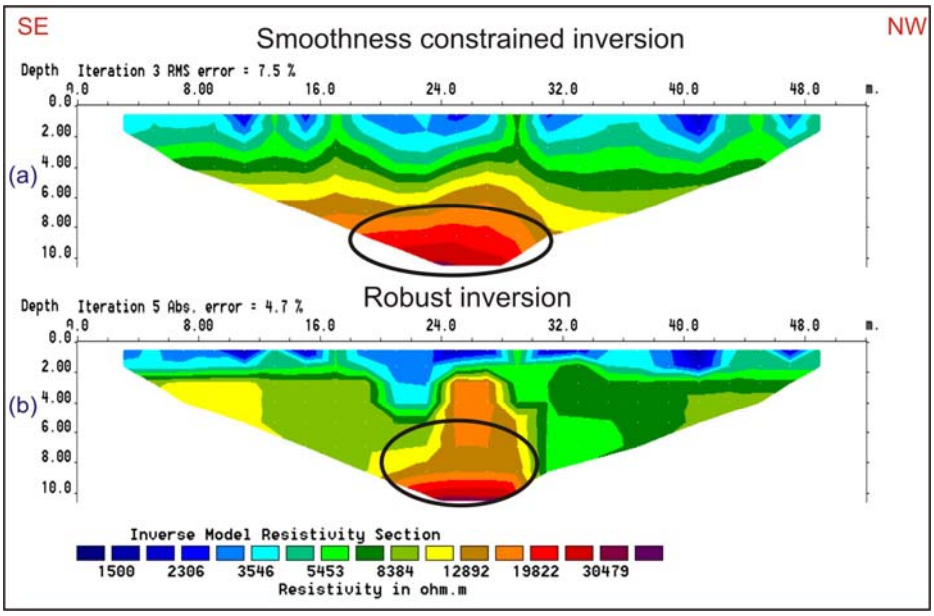

Fig. 9. Geoelectric section for line 5 using the smoothness constrained (a) and the robust (b) inversion.

CONCLUSIONS

The geological history of the whole area points out that the Permian-Triassic age sulfate deposit in Altsi has been subjected to deep-related transformations. More specifically, the dehydration of the primary gypsum to anhydrite occurred after burial, which resulted in the generation of a massive anhydrite volume. During the following exhumation, anhydrite came in contact with fluids of the active phreatic zone and the rehydration process began. The above setting contribute to the aspect that sulfate deposit in Altsi has experienced a HP/LT metamorphism (Dornsiepen et al., 2001) and nowadays is composed of an anhydrite core whose upper surface is hydrated to gypsum. In addition, the presence of rippled laminated gypsum in the pit indicates the increase of volume due to hydration, in correspondence to the process of direct hydration of anhydrite as has been suggested by Holliday (1970).

As for the efficiency of the geophysical survey, the 2D resistivity method proved to be a powerful tool to map the gypsum/anhydrite transition zone. The inversion results were confirmed by the existing data from boreholes and geological mapping. On the other hand, an anhydrite mass 10 meters in length and at least 6 meters high was detected in a sector of the mine that was believed to consist solely of gypsum.

The mixed array inversion of Wenner-Shlumberegr and Dipole-dipole array, in combination with electrode spacing up to 2.5 meters, gave the best results in locating lateral transitions of anhydrite to gypsum at shallow depths.

ACKNOWLEDGMENTS

The authors would like to thank Spyridakis Nikolaos, supervising engineer of Altsi open pit, for his technical support in field work, as well as two anonymous reviewers whose suggestions and comments improved the manuscript.

REFERENCES

Antoniou, M., 1987, Contribution to the knowledge of evaporitic deposits in Eastern Crete and Karpathos islands: *Mineral Wealth*, 49, 55-62, (in Greek).

Athanasiou, E., Tsourlos, P., Papazachos, C., Tsokas, G., 2007, Combined weighted inversion of electrical resistivity data arising from different array types: *Journal of applied geophysics*, 62 (2), 124-140.

Claebout, J., and Muir, F., 1973, Robust modeling with erratic data: *Geophysics*, 38 (5), 826-844.

DeGroot-Hedlin, C., and Constable, S., 1990, Occam's inversion to generate smooth, two-dimensional models from magnetotelluric: *Geophysics*, 55 (12), 1613–1624.

Derobert, X., and Abraham, O., 2000, GPR and seismic imaging in a gypsum quarry: *Journal of Applied Geophysics*, 45, 157-169.

Dornsiepen, U.F., Manutsoglu, E. & Mertmann, D. 2001, Permian – Triassic Palaeogeography of the external Hellenides: *Palaeogeography, Palaoeclimatology, Palaeoecology*, 172, 327-338.

Fytrolakis, N., 1980, The geological structure of Crete: *Habil. Thesis, NTUA, Athens*, 146 pages, (in greek).

Garcia-Ruiz, J. M., Villasuso, R., Ayora, C., Canals, A. and Ota´lora F., 2007, Formation of natural gypsum megacrystals in Naica, Mexico. *Geology* 35, 327–330.

Holliday, D. W., 1970, The petrology of secondary gypsum rocks: a review. *J. Sediment. Petrol.* 40, 734–744.

Kanaris, I., 1989, Gypsum deposits in the island of Crete: Internal Report IGME, Athens, 63 pages, (in Greek).

Papastamatiou, I., 1958, Report regarding Altsi gypsum deposit in Eastern Crete: Internal Report IGME, Athens, 3 pages, (in greek).

Pina, C. M., 2009, Nanoscale dissolution and growth on anhydrite cleavage faces. *Geochimica et Cosmochimica Acta*, 73, 7034–7044.

Rigakis, N. & Karakitsios, V., 1998, The source rock horizons of the Ionian Basin (NW Greece). *Marine and Petroleum Geology*, 15, 593-617.

Stummer, P., Maurer, H., and Green, A., 2004 Experimental design. Electrical resistivity data sets that provide optimum subsurface information: Geophysics, 69 (1), 120–139.

Trappe, Jorg, 2000, Pangea: extravagant sedimentary resource formation during supercontinent configuration, an overview: *Palaeogeography, Palaeoclimatology, Palaeoecology*, 161, 35–48.

Ulugergerli, E., and Akca, I., 2006, *Detection of cavities in gypsum*: Journal of The Balkan Geophysical Society, Vol. 9, No. 1, 8-19.

Ward, S., 1989, Resistivity and induced polarization methods: in Investigations in Geophysics No 5, Geotechnical and Environmental Geophysics, Vol. I, ed. S. Ward, SEG, Tulsa, 47-189.

Warren, John, 2006, Evaporites: Sediments, Resources and Hydrocarbons, pp. 1036, Berlin etc. (Springer).

Zhou, W., Beck, B., and Adams, A., 2002, Effective electrode array in mapping karst hazards in electrical resistivity tomography. Environmental geology, Volume 42, Number 8, p. 922-928.